Direct Fingerprint Classification in Raw Fingerprint Images by Using Principal Gabor Basis Functions

Chih-Jen Lee, I-Horng Jeng, Keng-Li Lin, Sern-Chiek Chew, and Lei-Shen Yueh
Department of Computer Science, Chinese Culture University, Taipei, Taiwan
{cjlee, zyh2}@faculty.pccu.edu.tw

ABSTRACT

A fingerprint classification algorithm can speed up the processes of fingerprint identification and verification. Therefore, this algorithm must be performed fast and correctly. Because Gabor filters only have large responses with similar orientation and spatial-frequency, in this paper, we will use a group of principal Gabor basis functions to represent the ridge structures of core regions. Fingerprint patterns will have large responses only to the Gabor filter-based templates of the corresponding classes. Therefore, the classes of fingerprints are directly detected from gray-scale images and many pixel-level computations are not involved. As a result, a fast class-detection for fingerprints is achieved.

1: INTRODUCTIONS

An efficient fingerprint classification algorithm can speed up the processes of fingerprint identification and verification. For fingerprint identification, the fingerprints with similar ridge structures are checked and the others are ignored. As for fingerprint verification, non-matching patterns are rejected as soon as possible if their ridge structures are different. So the ridge structures in fingerprints are very important for fingerprint identification and verification.

Based on the ridge structures in fingerprints, many approaches were proposed in [1-8]. In general, there are six types including arch, tented arch, left loop, right loop, whorl, and double loop. They are shown in Fig. 1. In [3], Wilson et al. combined whorl and double loop into one class. Therefore, the target types of fingerprint classification are five.

To classify the types of fingerprint, the number and the position of the cores and deltas are the most important features. In order to obtain the number and the position of the cores and deltas, the orientation map and Poincaré index were applied to judge whether the singular point exists (including cores and deltas) [2][4]. However, deltas points might disappear for some fingerprint capture devices. In [3][5], they used the orientation map as the features of neural networks to classify fingerprint patterns. But it might spend much time for training and it is not easy to propose a physical meaning to illustrate the weightings of networks. Cappelli et al. proposed a structure-based approach based on the orientation map in [6] and the syntactic approach also based on orientation map [1]. In order to obtain the orientation map, however, there are many steps involving pixel-level computation, such as image enhancement and gradient-based calculation. These steps are time consuming.

Gabor filters, simulating visual vertex cells, have the properties of spatial localization, orientation selectivity, and spatial-frequency selectivity [9]. Therefore, Gabor filters have been applied successfully and widely to many fields. In fact, each local fingerprint has its particular local ridge orientation (LRO) and local ridge frequency (LRF), and the whole fingerprint images are composed of various LROs and LRFs. In order to capture these intrinsic characteristics simultaneously, we proposed a local Gabor filter-based approach to determine the suitable Gabor filters over a complete set of Gabor filters by using only local information and then a local fingerprint is represented by a Gabor filter [10]. We also applied the selected Gabor filters, forming a template, to compare the similarity of two fingerprints directly from gray-scale image [11]. In [12], we also used a group of Gabor filters to simulate the core region; therefore, the core points are detected directly from gray-level images.

Based on the same concept, we will develop a Gabor filter-based approach to detect the class which belongs. The proposed approach can determine the results directly from gray-level images to avoid some time-consuming pixel-level computations.

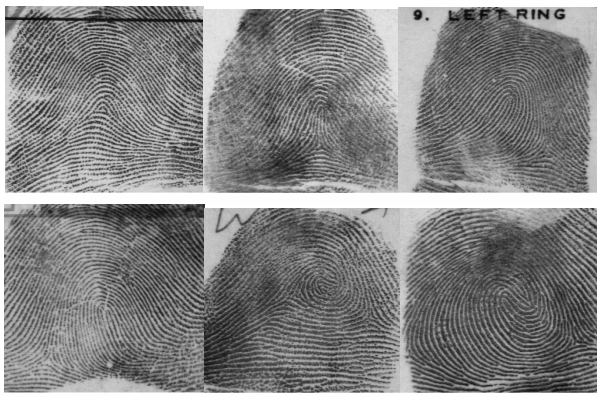

Fig. 1. Arch, tented arch, left loop, right loop, whorl, and double loop from left to right and top to button.

2: GABOR BASIS FUNCTIONS AND FINGERPRINT IMAGES

Gabor filters, simulating visual vertex cells, have the properties of spatial localization, orientation selectivity, and spatial-frequency selectivity. Therefore, we will apply Gabor filters to detect a particular local ridge orientation (LRO) and local ridge frequency (LRF) of a local fingerprint image.

2.1: GABOR BASIS FUNCTIONS (GBFS)

The two-dimensional (2-D) complete set of GBFs can be expressed as [10]:

$$G_{pqrs}(x,y) = \exp\{-[(x-p)^2 + (y-q)^2]/\sigma^2\} \exp[2\pi j(xr + ys)/N_f] \quad (1)$$

where $j = \sqrt{-1}$, $p, q = 0,1,\cdots,N_s - 1$, and $r, s = -N_f/2+1, -N_f/2+2, \cdots, -1,0,1,\cdots, N_f/2-1, N_f/2$. In the spatial domain, N_s is the number of spatial samples, (p,q) is the spatial window center, and σ decides the extent of spatial windows. In the spatial-frequency domain, N_f is the number of spatial-frequency samples and (r,s) is the location of the frequency center. The angle θ and radial frequency f of GBF are determined by $\tan^{-1}(s/r)$ and $\sqrt{(s/N_f)^2 + (r/N_f)^2}$, respectively. Their relationship on the spatial-frequency plane is demonstrated in Fig. 2. In Equation 1, we set the number of spatial samples, the number of spatial-frequency samples, and the extents of spatial windows along x and y axes as the same values for simplification. In the spatial domain, the real components of these basis functions for $N_s = N_f = 16$ are shown in Fig. 3. From Fig. 3, the orientation-selective properties of the GBFs are obvious. In the spatial-frequency domain, each real GBF (except $r = s = 0$) has twin Gaussian peaks. The envelope of Gaussian function, which is proportional to the reciprocal of σ, determines the channel bandwidths. In fact, each real GBF has twin Gaussian peaks at its frequency center (r,s). The complete GBFs spread $N_f \times N_f$ Gaussian peaks on the spatial-frequency plane. They only respond to the image with the same orientation and radial frequency as narrowband filters.

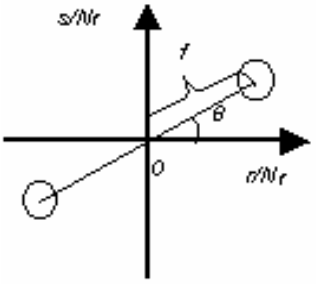

Fig. 2. Parameters of GBF on the spatial-frequency plane.

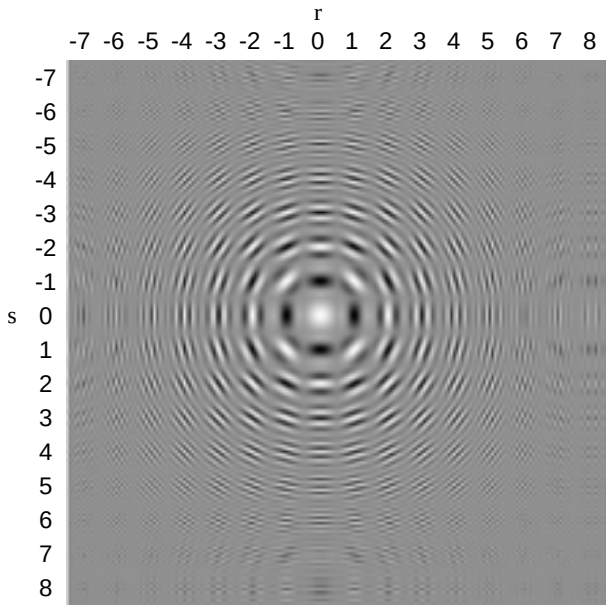

Fig. 3. The real components of the complete GBFs.

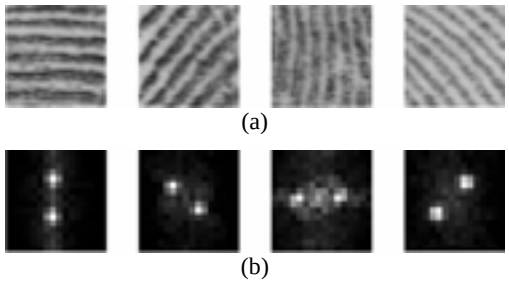

Fig. 4. (a) Original images and (b) responses of GBFs for various LROs.

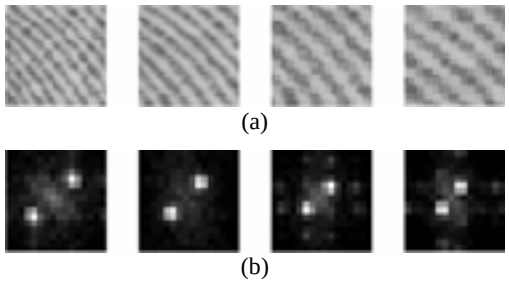

Fig. 5. (a) Original images and (b) responses of GBFs for various LRFs.

The Gabor response g of each GBF corresponding (r,s) is defined as follows:

$$g(r,s) = \left| \sum_{p}^{N_s} \sum_{q}^{N_s} I(x,y) G_{pqrs}(x,y) \right| \quad (2)$$

where I is an $N_s \times N_s$ input image. To demonstrate the relationship between GBFs and fingerprint images, some local fingerprint images with various LROs and LRFs are shown in Figs. 4(a) and 5(a), respectively. Figs. 4(b) and 5(b) show the corresponding Gabor responses from Figs. 4(a) and 5(a). From Figs. 4(b) and 5(b), the Gabor responses also have twin peaks, and the corresponding locations are similar to their Gabor coefficients. This means that the two corresponding

GBFs (in fact, they are the same) have the largest responses to the local fingerprint image. Moreover, the orientation and spatial-frequency of the corresponding GBF can represent mainly the local region because the image energy concentrates at its frequency. In other words, using only one GBF can easily capture the main characteristics of a local fingerprint image. We name it as the principal GBF (PBGF) of the local region which is defined by

$$g_M = \max_{r,s}[g(r,s)] \quad (3)$$

Because the PGBF can exactly capture the LRO and LRF of a local ridge structures, the dimension of a local fingerprint image is reduced from pixels to only one GBF. A GBF, determined by (r,s), can also be reduced to an index of the complete GBFs. If a local region has 16×16 pixels, for example, then there are 256 GBFs and the index of the PGBF needs only one byte. That is, the input feature vectors are reduced by a factor of 256.

2.2: PGBF TEMPLATE

Owing to the distribution of Gabor responses over the complete GBFs is similar to Gaussian distribution, larger response means the ridge structure is more similar to the corresponding PGBF. Therefore, we can distinguish the similarities of ridge structures according to the corresponding responses. After extracting the PGBFs of a whole fingerprint image, the image is viewed as the template of a group of LROs and LRFs, named PGBFs template. The second column of Fig. 6 shows the real components of the PGBFs template for non-overlapping sampling. To judge the similarity between the test image and the training pattern, we sample the test image directly from gray-scale by using the PGBF template of the training pattern. If the test image is similar to the training pattern, their responses of all sampling points are very close to each other. There is not necessary to extract PGBF for the test image. In Fig. 6, the third column shows the responses from self-PGBF template and the fourth from another. Their PGBF responses are very different.

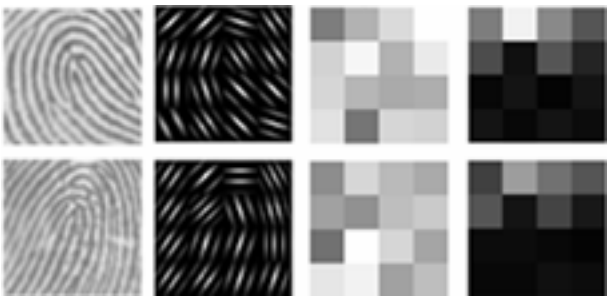

Fig. 6. From left to right: fingerprint images, PGBFs templates, Gabor responses from self-PGBFs template, and Gabor responses from another PGBFs template.

At last, the response of the PGBF template is defined by

$$R = \sqrt[N]{\prod_{i}^{N} \left| \sum_{p}^{N_s} \sum_{q}^{N_s} I_i(x,y) g_{Mi}(x,y) \right|} \quad (4)$$

where N is the number of the regions of interest.

3: CLASSIFIER DESIGN

As described in Section 2, we use a group of PGBF to form a particular ridge structures, then we can judge whether the raw fingerprint image contain the particular ridge structures. If the response is large, then the answer is yes. Therefore, we can avoid many pixel-level computations for orientation calculations.

Based on the above advantages, we will use a group of PGBF to form a particular class of fingerprint. Because every class has more than three subclasses, however, there are at least 15 possibilities of PGBF templates to represent the five classes of fingerprint. If a raw fingerprint image needs to compare all candidate PGBF templates, then the computational cost is high. So we develop a hierarchical structure to detect the corresponding class.

The proposed approach is shown in Fig. 7. There are three layers filters. The PGBF templates of the first layer detect the main direction below core point. There are four directions which are 0^0, 45^0, 90^0, and 135^0. They are shown in Fig. 8. After the detection for the main direction of core region, the PGBF templates of the second layer are applied to detect the belonging class according to the direction of the first layer. If the main direction of the pattern is 0^0, then there are two PGBF templates, shown in Fig. 8(a), to detect its corresponding class. The two PGBF templates are the classifiers of whorl and arch. If the main directions of the pattern are 45^0, 90^0, and 135^0, then there are four PGBF templates, shown in Figs. 8(a), 8(b), and 8(c), respectively. That is, there are at most four PGBF templates corresponding to each direction. The other PGBF templates need not to check.

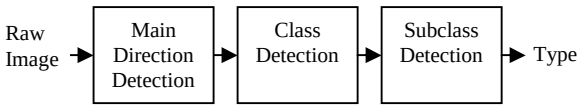

Fig. 7. The proposed approach.

Unfortunately, some left whorl and right whorl patterns might be classified into left loop or right loop. In the third layer, therefore, we use the PGBFs with 45^0 and 135^0, shown in Fig. 10, to detect right whorl and left whorl, respectively.

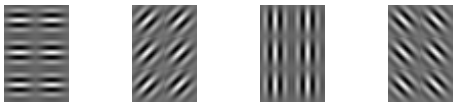

(a) (b) (c) (d)

Fig. 8. The first layer PGBF templates.

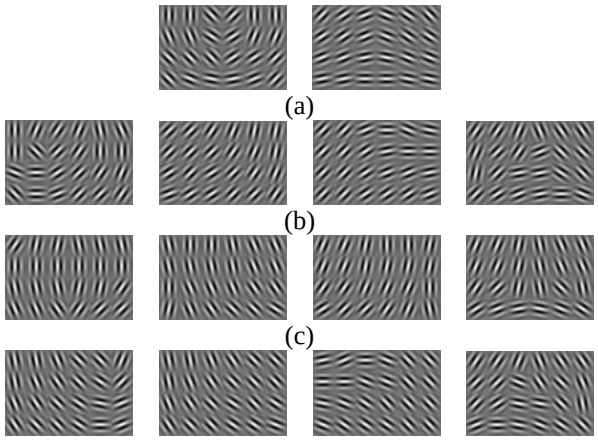

Fig. 9. The second layer PGBF templates connected to Fig. 8.

Fig. 10. The third layer PGBF templates.

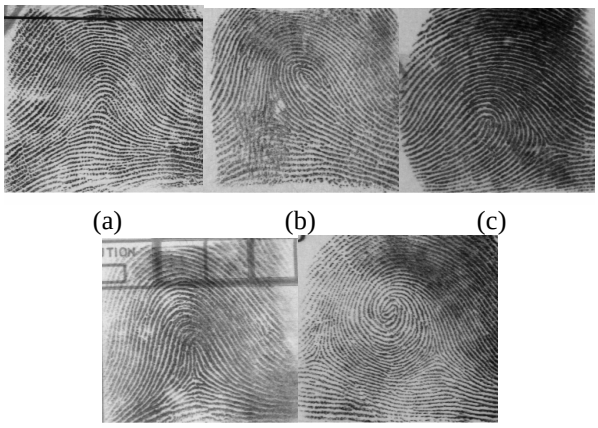

Fig. 11. Five types of fingerprints for test.

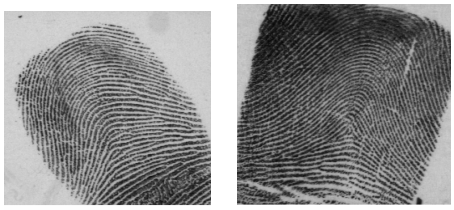

Fig. 12. Correct classification for rotated fingerprints.

Fig. 13. Some incorrect classification.

4: EXPERIMENTAL RESULTS

We use NIST Special Database 4 to test our approach [10]. The databases contain 4000 fingerprint images from 2000 fingers with 2 impressions. These images are scanned at about 500 dpi. In fact, the images sampled at 200~300 dpi is enough for extracting the LRO and LRF of a local fingerprint image. Therefore, we resample these images at 250 dpi. Not only memory space is reduced, but also the processing time is speeded up.

Fig. 11 shows five patterns belonging to five types, respectively. The values of each layer are shown in Table 1. These patterns are classified correctly. Fig. 12 shows some rotated patterns. They are also classified correctly. But some patterns are classified incorrectly. They are shown in Fig. 13.

5: CONCLUSIONS AND FURTHER RESEARCH

We have developed a fast algorithm to detect the classes of fingerprint patterns directly from gray-level images without preprocessing and other pixel-level computations. Based on the property that the Gabor filters only have large response with similar orientation and spatial-frequency, the ridge structures of core regions form a PGBF template. Observing the ridge structures of each class, we design a three-layer class detector. Therefore, the proposed method can directly detect core points from gray-scale images, and then faster than other pixel-level computation approach.

For fingerprint classification, conventionally, it is necessary to detect all singular points, including core points and delta points. In fact, the ridge structures of core regions can provide some clues for classification even though the delta points do not appear.

Testing with public fingerprint databases, such as the databases from NIST Special Database 4 and 14, is a very important task to show the ability of the proposed approach. We will use the some famous criteria to evaluate the performance of the Gabor filter-based approach.

Table 1. The results of Fig. 11.

Fig	1st layer				2nd layer					Class
11	45^0	90^0	135^0	0^0	A	T	L	R	W	
(a)	2035	1914	2672	5906	37667				5670	A
(b)	3419	1164	792	709	13505	3690	19935		13804	L
(c)	687	1311	5138	748	15540		10021	22468	16645	R
(d)	1423	2590	2355	1085		20331	13539	10665	7599	T
(e)	3591	1069	2744	2170	7206	9365	10050		16262	W

REFERENCES

1. Rao, K., Balck, K.: Type Classification of Fingerprints: A Syntactic Approach. IEEE Trans. Pattern Analysis Machine Intelligent, Vol. 2, No. 3. (1980) 302-314
2. Kawagoe, M., Tojo, A.: Fingerprint Pattern Classification. Pattern Recognition, Vol. 17, No. 3, (1984) 295-303
3. Wilson, C.L., Candela, G.T., Watson, C.I.: Neural-Network Fingerprint Classification. Journal of Artificial Neural Networks, Vol. 1, No. 2. (1994) 203-228
4. Karu, K., Jain, A.K.: Fingerprint Classification. Pattern Recognition, Vol. 29, No. 3. (1996) 389-404
5. Jain, A.K., Prabhakar, S., Hong, L.: A Multichannel Approach to Fingerprint Classification. IEEE Trans. Pattern Analysis and Machine Intelligent, Vol. 21, No. 4. (1999) 348-359
6. Cappelli, R., Lumini, A., Maio, D., Maltoni, D.: Fingerprint Classification by Directional Image Partitioning. IEEE Trans. Pattern Analysis and Machine Intelligence, Vol. 21, No. 5. (1999) 402 – 421
7. Park, C.H., Park, H.: Fingerprint Classification Using Fast Fourier Transform and Nonlinear Discriminant Analysis. Pattern Recognition, Vol. 38, No. 4. (2005) 495-503
8. Park, C.H., Lee, J.J., Smith, M. J.T., Park, K.H.: Singular Point Detection by Shape Analysis of Directional Fields in Fingerprints. Pattern Recognition, Vol. 39, No. 5. (2006) 839-855
9. Daugman, J.G.: Uncertainty Relation for Resolution in Space, Spatial Frequency, and Orientation Optimized by Two-Dimensional Visual Cortical Filters. J. Opt. Soc. Amer. A, Vol. 2, No. 7. (1985) 1160-1169
10. Lee, C.J., Wang, S.D.: Fingerprint Feature Reduction by Gabor Basis Function, Pattern Recognition, Vol. 34, No. 11. (2001) 2245-2248
11. Lee, C.J., Wang, S.D., Wu, K.P.: Fingerprint Recognition Using the Responses of Principal Gabor Basis Functions. Proceedings of Third International Conference on Information, Communications & Signal (2001)
12. Lee, C.J., Wu, K.P.: Fast Core Point Detection in Raw Fingerprint Image. Proceedings of the 17th Conference of Computer Vision, Graphics, and Image Processing (2004)
13. Watson, C.I., Wilson, C.L.: NIST Special Database 4, Fingerprint Database. U.S. National Institute of Standards and Technology (1992)